

## Slow positrons in single-crystal samples of Al and Al-Al<sub>x</sub>O<sub>y</sub>

K. G. Lynn and H. Lutz\*

*Brookhaven National Laboratory, Upton, New York 11973*

(Received 7 February 1980)

Well-characterized Al(111) and Al(100) samples were studied with monoenergetic positrons before and after exposure to oxygen. Both positronium-formation and positron-emission curves were obtained for various incident positron energies at sample temperatures ranging from 160–900 K. The orthopositronium decay signal provides a unique signature that the positron has emerged from the surface region of a clean metal. In the clean Al crystals part of the positronium formed near the surface is found to be associated with a temperature-activated process described as the thermally activated detrapping of a positron from a surface state. A simple positron diffusion model, including surface and vacancy trapping, is fitted to the positronium data and an estimate of the binding energy of the positron in this trap is made. The positron diffusion constant is found to have a negative temperature dependence before the onset of positron trapping at thermally generated monovacancies (>500 K), in reasonable agreement with theoretical predictions. The depth of the positron surface state is reduced or positronium is formed in the chemisorbed layer as oxygen is adsorbed on both Al sample surfaces, thus increasing the positronium fraction and decreasing the positron emission. At higher oxygen exposures [ $>500 \text{ L} (1 \text{ L} = 10^{-6} \text{ torr sec})$ ] positron or positronium traps are generated in the overlayer and the positronium fraction is reduced. The amorphous-to-crystalline surface transition of Al<sub>x</sub>O<sub>y</sub> on Al is observed between 650 and 800 K by the change in the positronium fraction and is interpreted as the removal of trapping centers in the metal-oxide overlayer. At the higher temperatures and incident energies vacancy trapping is observed by the decrease in the positron diffusion length in both the clean and the underlying Al of the oxygen-exposed samples. Similar vacancy formation enthalpies for Al are extracted in both the clean and oxygen-covered samples by a simple model and are in good agreement with those measured by other experimental methods. This technique provides a new experimental means for the study of interfaces and thin films and the vacancy-type defects associated with them.

### I. INTRODUCTION

Over the past 20 years positrons have been shown to be an effective probe for studying both vacancy-type bulk defects and the electronic structure of metals.<sup>1</sup> Most of these solid-state experiments have utilized energetic positrons obtained from radioactive sources and subsequently implanted well below the surface layer. After coming into thermal equilibrium ( $10^{-12}$  sec) with the metal a positron eventually annihilates ( $0.1\text{--}0.3 \times 10^{-9}$  sec), mainly with conduction electrons, emitting predominantly (>99%) two  $\gamma$  rays. In free space if a positron and electron are brought together a bound state called positronium (Ps) is formed. This bound state decays from either a singlet state,  $p\text{-Ps} ({}^1S_0)$  or triplet state,  $o\text{-Ps} ({}^3S_1)$ , each of which has unique annihilation characteristics.<sup>1</sup> Ps has not been found experimentally in metals, a fact which theoreticians ascribe to the screening of the Coulomb interaction between a positron and an electron.<sup>2</sup>

With the advent of slow positron beams<sup>3,4</sup> and the subsequent incorporation of these systems inside ultrahigh vacuum (UHV) chambers,<sup>5-7</sup> it is now possible to study surfaces with positrons. The unique signature provided by Ps enables one to detect when the positron leaves the surface region. At present one can, therefore, study the probability of Ps formation when a positron diffuses out of the metal as a function of sample temperature and incident positron energy. Whereas positron behavior is relatively well understood in the bulk, this is not true of positron interactions with even "well-characterized" surfaces.

The interaction of the positron at well-characterized surfaces has been partially revealed in recent studies. The positron can (i) be emitted into the vacuum without forming Ps,<sup>8</sup> (ii) escape with an electron and form Ps somewhere in the near-surface region,<sup>5-7</sup> or (iii) trap at a potential well at the surface and annihilate.<sup>9,10</sup> It is also possible for the positron to be thermally desorbed from the surface trap thus allowing Ps formation. From these processes and the use of a

simple model the depth of this trap can be estimated.<sup>9,10</sup> Recently a direct measurement of the velocity of these emitted Ps atoms has been performed on a Cu(111) surface.<sup>11</sup> At high temperatures two characteristic Ps energies were observed; one being associated with thermally desorbed positrons forming Ps and the other related to the kinetic energy distribution of Ps of  $3.4 \pm 0.3$  eV.

A number of fundamental questions still remain such as (i) the angular and energy distribution of the emitted positrons, (ii) the absolute branching ratio of each of these processes, and (iii) the effect of surface defects and impurities (possible activated sites). The above list is not exhaustive but should provide some of the information necessary to ascertain the usefulness of slow positrons in surface studies and the direction further studies might take.

In this work a simple metal (Al) is examined in the "clean state" and after a controlled amount of oxidation. The probability of Ps formation is measured as a function of incident positron energy and sample temperature on both the Al(100) and Al(111) surfaces before and after various oxygen exposures.<sup>12</sup> At different oxygen exposures a unique temperature dependence is observed in the Ps fraction relative to the clean samples. This unique behavior is associated with positron or Ps trapping sites located in the overlayer of amorphous aluminum oxide. A simple one-dimensional diffusion model originally proposed by Mills<sup>5</sup> and extended here, will be used in analyzing the Ps fraction data as a function of the incident positron energy. The fraction of those positrons emitted after implantation will also be briefly described.

The paper will be divided into the following: Sec. II experimental details, Sec. III theoretical discussion, Sec. IV slow-positron emission from Al(100) and Al(111), Sec. V Ps fraction versus incident energy at various sample temperatures, Sec. VI Ps-fraction measurements for Al(100) and Al(111) after exposure to oxygen, Sec. VII thermally activated detrapping of the positron from a surface state, Sec. VIII extraction of the vacancy formation enthalpy from the Ps data, and Sec. IX conclusions.

## II. EXPERIMENTAL DETAILS

The slow-positron apparatus used in these studies has been described elsewhere.<sup>6,13</sup> The present system employs split coils arranged in the Helmholtz condition for transport of the positrons to the target. UHV conditions are maintained throughout the apparatus during an experimental run. A Cu(111)+S crystal is used for the positron moderator.<sup>14</sup> When the moderator is first placed in the vacuum system, it is cleaned by Ar-ion bombardment. Annealing at 800°C removes the damage introduced by ion bombardment and diffuses S to the surface producing an

increased slow-positron yield. After this cleaning and heat-treatment procedure, the slow-positron yield can be maintained by simply heating the Cu to 750°C for approximately 10 min. The moderation efficiency, defined as the ratio of the slow-positron yield to the total yield of  $\beta$  decay positrons from a <sup>58</sup>Co source, is found to be approximately  $10^{-3}$ . With the present convertor design, the beam resolution is dependent on the extraction bias from the source region and is approximately 0.3 eV at an extracted positron energy of 20 eV. After collimation of the positrons to approximately 0.5 cm in both the *x* and *y* directions, the positrons can be accelerated into the sample at energies up to 10 keV by two consecutive five-stage electrostatic accelerators.

The Al single-crystal samples were mounted on 0.10-mm thick high-purity polycrystalline Ta foil, which was spot welded to Ta posts. Either a Pt, Pt/Pt-13% Rh, or a Cu/Constantan thermocouple was attached at the top of the crystal through a small hole produced by an electron discharge machine. A second thermocouple was mounted directly on the back of the supporting Ta foil. The counting electronics were gated off to remove any magnetic field effect generated when the current was passed through the Ta for heating of the Al crystals. For runs below 300 K a liquid-N<sub>2</sub> reservoir was attached to the top of a Ta post holder, cooling the sample by conduction. To keep the sample clean during a low-temperature run, a large-surface-area pump maintained at liquid-N<sub>2</sub> temperatures was mounted a few inches away from the target.

The positron work-function measurements<sup>13</sup> are made by a method similar to that of Mills *et al.*<sup>8</sup> In the present arrangement the retarding field is produced by a 97% transmission Cu grid on a movable arm to permit positioning in front of the sample. A 10-cm diameter stainless-steel plate is included behind the target to improve electric field homogeneity around the sample minimizing variations of contact potentials produced by different materials in the sample region.<sup>13</sup> The grid is kept at +4.69 V while the sample voltage is ramped from 0 to 10.31 V. During these runs -20 V is applied to the accelerators to ensure that the source is totally absorbent to the emitted positrons. When the target is biased more positively than the grid the emitted positrons will travel back towards the source, however, when the target is more negative than the grid only those positrons with a kinetic energy greater than the difference in the applied voltages will escape the target region. Those positrons which annihilate in the target region are detected and the data recorded with a multiscaler as a function of target bias. In all of these measurements the sample was perpendicular to the applied magnetic field axis to remove the dependence of  $\theta$  (angle of the sample to the axis of the magnetic field) on the emitted positron energy distri-

bution. The annihilation photons were measured using a Ge(Li) radiation detector with a resolution of 1.35 keV full width at half maximum at a photon energy of 514 keV produced by a  $^{85}\text{Sr}$  source.

When Ps atoms form, the statistical weight should produce three times as much *o*-Ps ( $^3S_1$ ) as *p*-Ps ( $^1S_0$ ). The  $^1S_0$  state primarily decays into two photons with the energy of each photon approximately equal to  $m_0c^2$  (511 keV). The  $^3S_1$  decays mainly into three photons and each photon ranges in energy from approximately 0 to  $m_0c^2$ , where the sum of the energies of the three photons equals  $2m_0c^2$ .<sup>15</sup> If *o*-Ps forms in a condensed medium (i.e., molecular materials), the probability of decay into three photons is reduced by a pickoff process whereby a surrounding electron having an opposite spin annihilates with the positron producing two photons. The measured energy spectrum of those *o*-Ps atoms decaying by three photons is markedly different from the two-photon process obtained when positrons annihilate in the bulk metal. By simply measuring the change in the observed  $\gamma$ -photon energy spectrum one can estimate the fraction ( $F$ ) of Ps produced if one assumes the statistical weight of 3 to 1. If one has energy spectra representing 0% Ps and 100% Ps then the intermediate fractions can be extracted by a method first used by Marder *et al.*<sup>16</sup> and initially applied to slow-positron studies by Mills.<sup>5</sup>

In these measurements the 0% Ps limit ( $F = 0$ ) was obtained by measuring the energy spectrum in Al(100) at 900 K with an incident positron energy of 5 keV. From an earlier work by Lynn,<sup>10</sup> it was found that thermally generated vacancies, which are known to trap positrons,<sup>1</sup> drastically shorten the positron diffusion length; therefore almost all of the positrons are trapped at these defects and only a very small percentage can escape the solid and form Ps. An extrapolation procedure was performed by fitting a third-order polynomial to the high-temperature Ps fraction data versus incident energy thereby providing the actual  $F = 0$  limit. When a  $^{68}\text{Ge}$  source was sealed between two pieces of Al and inserted in the UHV chamber, this  $F = 0$  Ps limit was confirmed. The two methods agreed to within approximately 10% of each other, although backscattering of the annihilation photons was important in deducing the correct  $F = 0$  limit with the sealed  $^{68}\text{Ge}$  source. Background subtraction was also necessary for the sealed source.

It was assumed that a 100% Ps signal was produced when low-energy positrons ( $\sim 20$  eV) impinged on a hot Al crystal ( $> 900$  K). These low-energy positrons do not show signs of trapping at thermally generated vacancies at high temperatures. Other researchers<sup>5,7</sup> have used a hot Ge target for the 100% Ps fraction calibration point and this work appears to be a few percent higher than the fraction obtained using hot Al. It is assumed that none of the *o*-Ps formed while leaving the surface undergoes a spin-

exchange process. Some fraction of *o*-Ps atoms do however suffer wall collisions before decaying in the vacuum, thus undergoing spin exchange and then decaying by two photons. This fraction depends upon the spatial and energy distribution of the emitted Ps atoms and the spatial arrangement of the target in the vacuum chamber.<sup>13</sup> A small calibration error is produced, however, this effect has been minimized by placing the sample in an open region. Reasonable agreement between the hot Al results and those generated by convoluting the theoretical energy distribution of both the  $^1S_0$  and  $^3S_1$  with the detector resolution for the 100% Ps limit was obtained.

During either the positron work function or the Ps fraction studies the sample could be rotated for examination using low-energy electron diffraction (LEED) or Auger electron spectroscopy (AES) measurements. The pressure was kept below  $2 \times 10^{-10}$  torr during all of the positron measurements. No ionization gauge was in a direct line of sight of the sample and the existing nude gauge in the UHV chamber was only used during the oxygen exposures.

LEED and AES measurements were performed using a standard Varian four-grid LEED optics. Primary electrons at normal incidence to the Al crystals were used. The beam energy was varied for the LEED experiments between 60–300 eV, and kept at a constant of 3 keV for the AES measurements. AES experiments were also performed with a glancing incident gun and similar results were obtained.

The 99.999% Al crystals purchased from Materials Research Corporation and oriented to ( $\pm 2^\circ$ ) in the (111) and (100) planes were mechanically polished and etched before insertion into the vacuum chamber. The samples were outgassed for 24 h at 400 °C before the initial cleaning procedure. The samples were cleaned by repeated cycles of Ar-ion bombardment ( $\sim 200$  °C) and annealed (400 °C) for at least 30 min until no oxygen signals were observed by AES.<sup>17</sup>

### III. THEORETICAL DISCUSSION

A one-dimensional diffusion model was first applied by Mills<sup>5</sup> to describe the Ps fraction as a function of the positron incident energy. In these experiments the quantity of interest is the number of positrons which diffuse back to the surface after implantation, before trapping at some defect or annihilating at a rate corresponding to that of a so-called "defect-free" metal. The equations that were fit to the Ps fraction data will not be described in detail as they have been discussed by Lynn and Welch<sup>18</sup> and more recently by Mills and Murray.<sup>19</sup> However, a brief explanation of the modifications to these equations will be given. Up to the present time, the Ps data

have only been fitted when an exponential stopping profile with a mean depth linear in the incident energy was assumed.

Mills and Murray<sup>19</sup> have theoretically considered a more complicated stopping profile, although no comparison was made to experimental data. This approach employed a positron stopping profile proposed by Makhov<sup>20</sup> for electrons. No assumptions are needed about the mean depth being linear in  $E$ . The scheme does have the undesirable effect of producing a nonanalytical form for the final equation. Although this approach is philosophically attractive, more fitting parameters are needed and strong correlations exist between these fitting parameters, therefore producing large uncertainties in the extracted values. In the present model a simple modification has been made to the exponential stopping profile. This approach produces a better representation of the experimental data and can be solved in closed form.

In this derivation one assumes that the normalized initial positron distribution,  $C_0(x)$ , is of the form

$$C_0(x) = \frac{e^{-x/\bar{a}}}{\bar{a}}, \quad (1)$$

where  $\bar{a}$  is the mean depth of implantation. One can then take the mean implant depth on energy in the form of  $\bar{a} = E^\alpha/A$ , where  $A$  is the constant relating the mean positron depth to the incident energy. Following an approach similar to Refs. 18 and 19 one can then derive the expression for the Ps fraction

$$F = \frac{f_0}{1 + (E/E_0)^\alpha} \quad (2)$$

In the above equation,  $E$  is the incident positron energy,  $f_0$  is the Ps fraction at  $E = 0$  for a perfect reflector and absorber, and  $E_0^\alpha = (D\tau_{\text{eff}})^{1/2}/A$ , where  $D$  is the positron diffusion constant, and  $\tau_{\text{eff}}$  is the effective positron lifetime. In Eq. (2),  $E_0$ ,  $f_0$ , and  $\alpha$  are the adjustable parameters, although one can easily estimate  $f_0$  from the experimental low-energy Ps fraction data. By including  $\alpha$  as a fitting parameter a much improved fit to the data was found. Furthermore, convergence in the fit was easily obtainable in all cases. In fact, the correlation between the fitting parameters<sup>21</sup> decreased, thereby producing smaller error bars on the extracted values. As shown by Refs. 18 and 19, Eq. (2) is valid for a partially transmitting boundary, as one might expect is the case for an extended Bloch-like positron approaching the surface from within the crystal. Other temperature-independent positron distribution profiles have been employed which produce different functional forms than Eq. (2), although the same general features of  $f_0$  and  $E_0$  are found. Fitting the data with the different functional forms one finds that  $E_0$  does vary in absolute magnitude, although the temperature dependence of  $E_0$  is found to be almost independent of the

initial positron profile. One might expect some variation in the initial positron distribution profile with temperature owing to positron-phonon scattering.<sup>22</sup> When solving the diffusion equation utilizing the radiative boundary condition as discussed in Ref. 19,  $f_0$  in Eq. (2) is equal to

$$f_0^* = f_0/[1 + B(D\tau_{\text{eff}})^{1/2}],$$

where  $B$  equals  $\infty$  for a reflecting boundary and 0 for an absorbing boundary. In a recent work<sup>22</sup> where both the conduction electron and phonon scattering were taken into account for calculating the mean penetration depth for the positron, it was determined that as the incident energy is increased above 1 keV in Al the penetration depth becomes more peaked thus changing the exponential distribution. As Mills *et al.*<sup>8</sup> have indicated, Eq. (2) can also be fit to the yield of positron emission curves as a function of incident energy.

After fitting Eq. (2) to the Ps fraction versus incident positron-energy data one can easily observe that  $E_0$  decreases at the higher temperatures, which has been explained by positron trapping at thermally generated monovacancies.<sup>5,10</sup> If one assumes that the monovacancies are in thermal equilibrium and are the predominant trapping centers, the fitting equation as shown by Lynn and Welch<sup>18</sup> is

$$E_0(T) = \frac{A(D\tau)^{1/2}}{[1 + \tau\mu \exp(S_{\text{V}}^f/k) \exp(-E_{\text{V}}^f/kT)]^{1/2}}, \quad (3)$$

where  $\mu$  is the monovacancy specific trapping rate,  $\tau$  is the positron lifetime for a freely diffusing positron in Al, and  $S_{\text{V}}^f$  and  $E_{\text{V}}^f$  are the monovacancy formation entropy and enthalpy, respectively. This equation was derived by assuming an effective annihilation rate, which should be a good approximation for trapping if the intertrap spacing is small compared with the scale of the spatial variation of the initial positron probability distribution. Furthermore, this equation assumes that once a positron is trapped, it has a negligible probability of escaping the vacancy before annihilation. In bulk positron measurements no detrapping of positrons from monovacancies in Al has been observed.<sup>1</sup> In the present studies there may be a finite probability that the positron trapped at a vacancy near the surface could tunnel into the surface state and detrapp, thereby forming Ps. The temperature dependence of  $E_0$  extracted from the original Ps fraction data is then fitted with three parameters which are defined as  $E_0(0) = A(D\tau)^{1/2}$ ,  $U = \tau\mu$

$\times \exp(S_{IV}^f/k)$ , and  $E_{IV}^f$ . Therefore Eq. (3) becomes

$$E_0(T) = \frac{E_0(0)}{[1 + U \exp(-E_{IV}^f/kT)]^{1/2}} \quad (4)$$

One can eliminate  $E_0(0)$ , as it represents the low-temperature fits of the original data. A small error is included, as there is a predicted  $T^{-1/2}$  behavior for the positron diffusion constant in metals.<sup>23</sup> This temperature dependence will be discussed in more detail later in the paper.

One increases the surface sensitivity of the positron by lowering the incident energy to a point where trapping at thermally generated monovacancies is not observed. This ensures that almost all of the positrons interact with the surface region, therefore making it possible to study the temperature dependence of the Ps fraction in the surface region. The ability of the incoming positron to directly form a stable Ps atom when above a few electron volts is assumed to be negligible. In general the positron in the surface region may escape as a free positron, trap at a potential well at the surface, or escape as Ps. Once trapped at the surface the positron can either annihilate or be thermally activated out of this surface state, forming Ps while escaping. The temperature dependence of these branching ratios can be experimentally measured, although presently no theoretical predictions exist on either of the relative fractions. Certainly, the electronic structure, surface defects, impurities, and crystallographic planes play a role in these processes.

Thermally activated detrapping has been observed in both metals<sup>9,10</sup> and semiconductors.<sup>9</sup> Surface-state models have been proposed by different researchers,<sup>24</sup> and appear to describe the general features found experimentally. Our data showing this detrapping phenomena are analyzed in a manner described by Lynn and Welch,<sup>18</sup> and brief comparisons to other results will be made in Sec. VII.

The observed temperature dependence of detrapping, assuming a single activation energy, is described by

$$\Gamma_{em,t} = \nu \exp(-\Delta E/kT) \quad (5)$$

where  $\Gamma_{em,t}$  is the rate at which trapped positrons are emitted into the vacuum,  $\nu$  is the frequency of the bound positron in the surface state times a probability of forming Ps, and  $\Delta E$  is the activation energy. In this derivation  $\nu$  is assumed to be temperature independent. Following the derivation of Lynn and Welch,<sup>18</sup> the temperature dependence of the branching ratio,  $f_0$ , becomes

$$f_0 = \frac{[C_1 + \exp(-\Delta E/kT)]}{[C_2 + \exp(-\Delta E/kT)]} \quad (6)$$

where

$$C_1 = m\Gamma/\nu \quad (7a)$$

$$C_2 = \Gamma/\nu \quad (7b)$$

$m$  is the fraction that is initially emitted as Ps at low temperatures, and  $\Gamma$  is the annihilation rate of positrons trapped at the surface. The value of  $m$  should be an intrinsic property of the surface and it is found to be extremely sensitive to surface impurities, as will be discussed. For a general derivation of Eq. (6) the reader is referred to Lynn and Welch.<sup>18</sup> The physical interpretation of  $\Delta E$  is made uncertain by the lack of a detailed understanding of the particular mechanism by which the positrons are emitted and form Ps. Mills<sup>9</sup> has applied a Born-Haber cycle, including this activation energy, whereby the binding energy of the positrons to the surface trap,  $E_{ST}$ , can be deduced. As discussed by Mills<sup>9</sup> and by Lynn and Welch<sup>18</sup> the expression is

$$E_{ST} \leq \Delta E + 6.8 - \Phi_e \quad (8)$$

where  $\Phi_e$  is the measured electron work function and the 6.8 (given in terms of eV) is the gain in energy when Ps forms. One should remember that this model does not include any inelastic processes which occur or any prediction on the fraction of Ps or positrons which escape at low temperatures. The Ps atom, when escaping the surface region, does need to surmount a weak induced dipole-dipole interaction, i.e., van der Waals attraction to the metal surface. A positron diffusing to the surface from the interior, if not reflected, must proceed across the metal-vacuum interface in on the order of  $10^{-14}$ – $10^{-15}$  sec to avoid being trapped by this surface state. Nieminen and Lakkonen<sup>25</sup> have estimated the trapping rate into a planar surface state as  $7.6 \times 10^5$  cm/sec. Assuming a width of the surface state of 3 Å, one finds a transition rate of  $2 \times 10^{15}$  sec<sup>-1</sup>, consistent with what one should expect if some of the positrons can escape without trapping. It is important to note, that this calculated value<sup>25</sup> of the trapping rate is only an approximate number as the surface-state parameters are not accurately known. One would expect that the more negative the positron work function (larger escape velocity), the fewer the number of positrons that would trap in the surface state or form Ps while escaping the surface. It should be mentioned that the positron reflection coefficient could become larger the more negative the positron work function. The positron could also lose energy and momentum in a short time by Auger excitations thus becoming trapped in the surface state. Presently no calculation has been performed on the likelihood of this process.

The Ps work function,  $\Phi_{Ps}$  is defined as the energy required to remove a nontrapped thermalized positron from a metal without stripping the electron correlation cloud. This can be estimated by a Born-

Haber cycle assuming no inelastic processes and is represented by

$$\Phi_{Ps} = \Phi_3 + \Phi_p - 6.8 \quad (9)$$

again in eV. For most metals, other than the alkalis and Pb,  $\Phi_{Ps}$  turns out to be negative as the sum of  $\Phi_e + \Phi_p$  is usually less than 6.8 eV. In all clean annealed metals studied to date Ps is found to emerge, indicating a negative Ps work function in agreement with theory.<sup>26</sup> A measurement of the kinetic energy of Ps made by Mills and Pfeiffer<sup>11</sup> appears to provide support for this simple picture of the physical process of escape. This study certainly had a large fraction of nonthermal positrons forming Ps, therefore any conclusions reached concerning the measured energy distribution must take account of the nonthermal fraction. When Ps is formed from a thermalized positron and escapes the surface one would expect that inelastic processes might be important in producing a slightly lower energy than predicted by Eq. (9). The exact process by which the binding energy of Ps is converted into the kinetic energy of the escaping Ps has not been dealt with to the authors' knowledge, but one possibility is that the excess energy could be given to a spectator electron or phonons. The exact escape process of Ps awaits further experimental and theoretical work.

More recently, Pendry<sup>27</sup> has considered the surface state as a mixed positron-Ps entity trapped between the vacuum and solid. This mixing can occur between the positron and Ps because a conversion can take place by the exchange of an electron with the surface. In this model Pendry predicts that Ps should be emitted, preferentially normal to the surface with a discrete energy, however, the sharp vacuum-metal interface ionizes some fraction of the Ps allowing the emitted positrons to be distributed over a range of angles and energies. This model alleviates the necessity for the positron to emerge from the solid without being trapped at the surface. Further experiments have been made to delineate between these possibilities, however, further discussion of these models is beyond the scope of this paper.

#### IV. SLOW-POSITRON EMISSION FROM Al(100) AND Al(111)

Emission of a thermalized positron occurs in those metals which exhibit a negative positron work function,  $\Phi_p$ , favorable for emission into the vacuum.<sup>26</sup> With this interpretation, as previously mentioned, the positron must cross the metal-vacuum interface without being trapped in the surface state. The fraction of positrons that escape without being trapped or forming Ps should depend on the magnitude of the work function, the details of the potential well, and

therefore the electronic structure of the surface. Because of the low implant energies ( $\sim 2$  keV) some of the positrons will not be fully thermalized and can be seen as the rounding in Fig. 1.

Figures 1(a) and 1(b) show the integral energy spectra of the slow-positron ( $e^+$ ) yield from a single

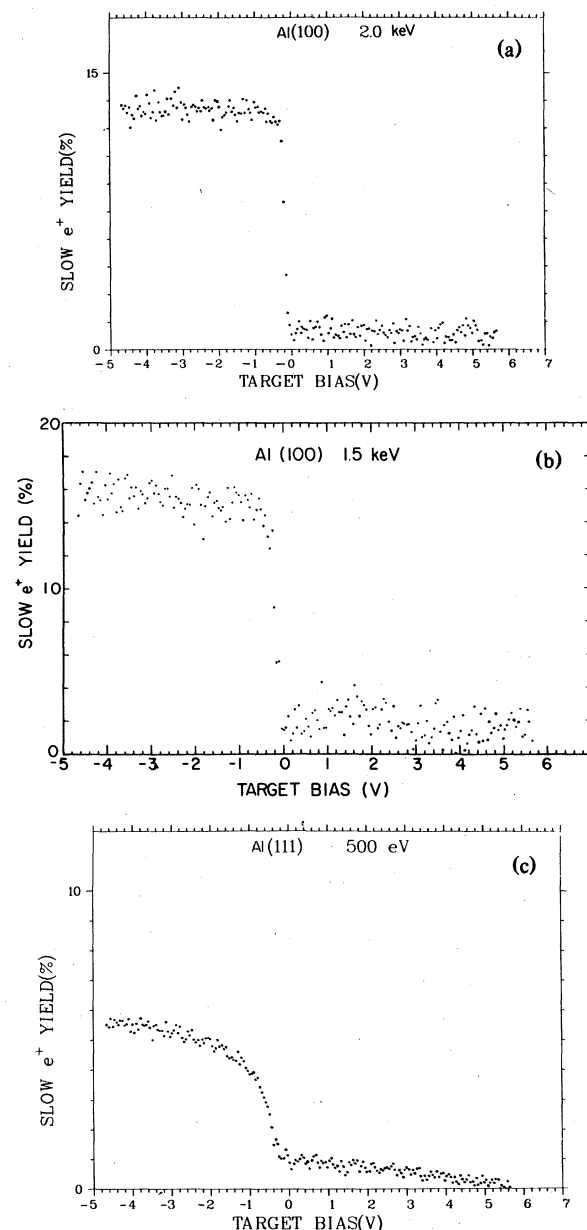


FIG. 1. Retarding-potential spectra of the slow-positron emission at 298 K of (a) Al(100) with a 2.0-keV incident positron energy, (b) Al(100) with a 1.5-keV incident positron energy, (c) Al(111) with a 500-eV incident positron energy. All these spectra have had a linear background subtracted. The slow-positron yield is the ratio of the number of reemitted positrons to the total number incident on the target.

crystal of Al(100) for two incident positron energies, 2.0 and 1.5 keV at 298 K. The slow-positron yield is defined to be the ratio of the number of reemitted positrons to the number incident on the target. The target bias is experimentally measured with respect to a positively biased Cu grid in front of the sample. It is worth mentioning that the voltage where the rise occurs in Figs. 1(a), 1(b), and 1(c) is a measurement of the contact-potential difference between that of the particular sample and the positively biased Cu grid. The width ( $\Delta E_{wp}$ ) of the steep rise, as seen in Fig. 1, is the integral longitudinal ( $\frac{1}{2} m v_{11}^2$ ) energy spectrum of the slow positrons emitted by the target.<sup>8</sup> The width of the decrease in the yield is a direct measurement of the energy and angular spread of the emitted positrons. This width ( $\Delta E_{wp}$ ) for the Al(100) is on the order of 0.2 eV, in good agreement with Mills *et al.*<sup>8</sup> For the Al(111), Fig. 1(c), it is difficult to determine the width of the curve, however, other experiments at higher incident energies indicate that the energy spread of the emitted positrons is  $+0.1 \pm 0.10$  eV with a yield of approximately 10% at 300 K. Variations in the yield were observed for different Al(111) samples but were consistently 10% or less. Careful annealing of the samples to remove various positron trapping centers was found to be necessary before work-function measurements were made. Differences in the slow-positron yield were also found on various Al(100) surfaces even when the AES showed no impurities. This may also be an indication of the possible presence of chemisorbed H, which cannot be detected by AES, or possibly surface roughness. The theoretical calculations of Hodges and Stott<sup>26</sup> predict a positive sign ( $\Phi_p = +0.7$  eV) for the positron work function on Al, contrary to our experimental findings.

As one lowers the incident positron energy a larger fraction of nonthermal positrons escape the metal thus causing a rounding of the emission curve. This can easily be seen in Fig. 1(c) for the Al(111) crystal with an incident positron energy of 500 eV. Even though complete thermalization is theoretically predicted to occur in the order of  $\sim 10^{-12}$  sec in Na, there is some probability that a fraction of these incident slow positrons will escape without becoming fully thermalized in the metal. In a review by Bergersen and Pajanne<sup>28</sup> energetic positrons are shown to reach the eV range after  $\sim 10^{-14}$  sec and to become fully thermalized in the order of  $10^{-12}$  sec. For low-energy incident positrons ( $\sim 500$  eV), assuming a range of less than 75 Å, one can easily show that a small fraction will not be thermalized before reaching the surface from the interior.

The slow-positron yield is found to be both incident energy and temperature dependent, in agreement with Mills *et al.*<sup>8</sup> The slow-positron yield is determined by taking the difference between the integral of the counts from  $-1.67$  to  $-3.44$  V and the

integral of the counts from 0.34 to 2.11 V divided by the integral for the former. In this study a slightly higher yield of slow positrons is found compared to Mills *et al.*<sup>8</sup> which can be attributed to variations in the cleanliness and possibly surface roughness of the samples. Both positron emission and Ps formation at crystal surfaces are thought to be affected by kinks, surface vacancies, or grooving. Further experiments are needed to determine which surface defects play a role. Since our results are in reasonable agreement with Mills *et al.*<sup>8</sup> they will be only briefly discussed. In Al, oxygen decreases the slow-positron yield, although in other metals one can increase the yield and the magnitude of the positron work function when certain impurities are present.<sup>9,13</sup>

The ability of some fraction of the positrons to escape the surface trap and emerge into the vacuum can be understood in terms of a transition-limited trapping process. Even though the positron work function is negative in Al there will be quantum-mechanical reflections of a positron approaching the one-dimensional barrier from within the metal. This has been recently treated theoretically by Oliva,<sup>22</sup> where thermal energies ( $\sim 0.03$  eV) are small compared to the barrier height for positrons (0.1–1.0 eV) and Ps (2–3 eV). If these surface traps are deep ( $E_{ST} > 1$  eV) one would expect that the positron would lose its energy predominantly by electron-hole generation or Auger excitations. The width of the surface state, the energy-loss mechanisms, the medium, and the positron wave function mainly determine the ability of the positron to escape the surface trap. The role of the phonon-mediated loss process has been determined by Nieminen and Lakkonen<sup>25</sup> to be small and only slightly temperature dependent. Without considering the internal reflection of the positron and with the above interpretation of transition-limited trapping one would expect a higher yield with a more negative positron work function as the positron traverses the surface state more rapidly and can escape the sample. This appears to be in general agreement with our results.

Figure 2 shows the variation in the yield as the sample temperature is increased. Mills *et al.*<sup>8</sup> have associated this decrease in the yield with an activated process and fit the data by an Arrhenius plot with an activation energy of  $0.68 \pm 0.02$  eV. These researchers initially suggested that positron trapping at bulk thermally generated vacancies was responsible for the decreasing yield. Bulk positron-lifetime measurements were made by us on similar crystals. From these measurements it was found that no significant fraction of the positrons was trapped until approximately 75°C higher than the initial decrease shown in Fig. 2. Moreover, the bulk measurement was consistent with other results of this type,<sup>1</sup> indicating that these bulk vacancies are not responsible for the change in the yield. This result is interpreted as evi-

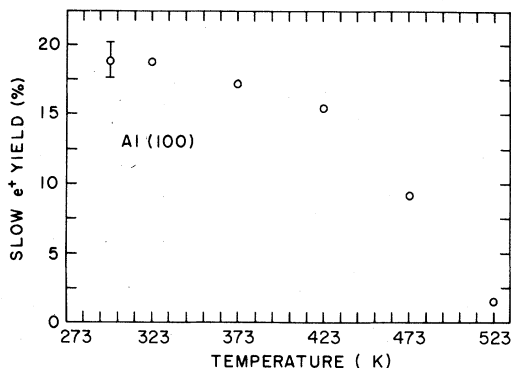


FIG. 2. Slow-positron yield (%) vs Al(100) temperature for a 1-keV incident positron energy.

dence that the branching ratio changes for Ps relative to free positrons. Similar behavior in the Al(111) crystal was found, although the yield starts to decrease at a lower temperature and approaches zero at 400 K. The findings for Al(100) are in rough agreement with Mills *et al.*,<sup>8</sup> although one can fit the results with a simple negative temperature dependence which could be associated with the positron work function becoming less negative. There have not been any calculations on the expected temperature dependence of the positron work function. The temperature dependence of the positron work function should depend (similar to the electron work function) on the following effects: (i) volume expansion of the lattice, (ii) variation of the dipole layer, (iii) particle-lattice coupling, and (iv) electronic specific heat. Positron-emission measurements have also been performed on the Al(100) sample down to temperatures of 165 K with little change in the width of the curves. The Al(111) results show that a significant increase ( $\sim 5\%$ ) in the slow-positron yield occurs between 180 and 300 K. These Al(111) measurements can be represented by a negative temperature dependence of the positron work function which changes the yield of emitted positrons. This absence of emission at the higher temperatures could then be associated with the change in sign of the positron work function. More detailed experiments will have to be performed to confirm this possibility.

#### V. Ps FRACTION VERSUS INCIDENT ENERGY AT VARIOUS SAMPLE TEMPERATURES

Detection of Ps ( $^3S_1$ ) decay provides a unique signature which indicates that a positron has passed through the metal-vacuum interface. Understanding this process should produce new information about

the electron distribution at the surface. As discussed in an earlier section, a quantitative measure of the Ps ( $^3S_1$ ) fraction decaying by three photons in clean metals can be made simply by measuring the changes that occur in the energy spectrum of the annihilation photons. In the present measurements the samples were negatively biased to produce the desired incident energy, therefore the emitted positrons were attracted back to the target and partially converted into Ps. This has the effect of producing an overestimate of the absolute Ps fraction. For example, at 300 K Al(100) is found to emit  $\sim 20\%$  slow positrons for 1-keV incident positrons. If one assumes that of those emitted positrons attracted back to the negatively biased sample 50% form Ps and the remaining positrons become trapped in the surface state and annihilate, then the measured Ps fraction would be overestimated by  $\sim 10\%$  of the total flux. An overestimation in the absolute Ps fraction on the order of 12% would be possible at the lower incident energies. At the lowest positron energy, where the overestimation is largest, the incident energy was varied from the source and the target was grounded allowing those emitted positrons to escape. At high incident energies or high sample temperatures ( $>300^\circ\text{C}$ ) the slow-positron yield decreases, therefore this relative error in the extracted Ps fraction is very small. It should be noted, that only a small correction is necessary for the Al(111) sample as there is a low yield of emitted slow positrons ( $<1$  eV).

Figure 3 shows the Ps fraction,  $F$ , versus the incident positron energies for Al(111) at various sample temperatures. The lower-temperature data are

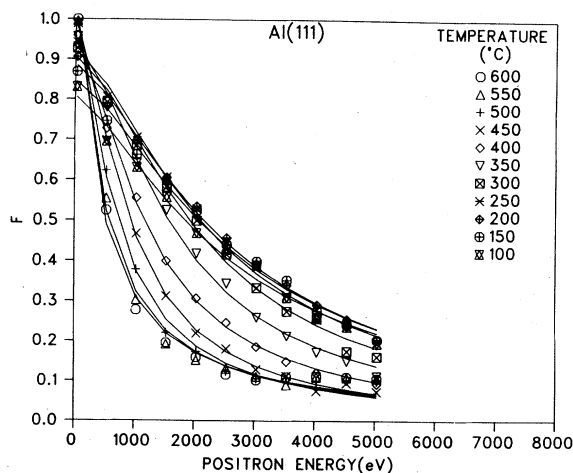


FIG. 3. Ps fraction for Al(111) as a function of incident positron energy. The solid lines are the best fit of Eq. (2) through the data. No impurities were observed with AES measurements and a sharp LEED pattern was observed. The statistical error bars are approximately the size of the data points.



not included in Fig. 3 for clarity. The solid lines are the result of the least-squares fitting of Eq. (2) to the experimental data. A much poorer fit is obtained and convergence is more difficult when  $\alpha$  in Eq. (2) is constrained to be 1, as in the case of the previous model.<sup>5</sup> The effect of positron trapping at thermally generated monovacancies can be observed at higher implant energies by the large decrease in the fraction of those positrons which reach the surface and form Ps. In other words, the effective diffusion length for the positron is shortened.

The fitted values of  $E_0$  determined in the temperature range from 160 to 500 K for Al(100) produced a  $T^{-0.38 \pm 0.05}$  dependence. An implicit assumption was made in our analysis which is that there is no temperature dependence on the range of the positrons in this temperature region. The bulk positron lifetime only changes a few percent over the temperature range studied, therefore this should not produce a significant effect on  $E_0$ .<sup>18</sup> A calibration error in  $F$  or more specifically in  $R_0$  or  $P_1/P_0$  can have a significant effect on the temperature dependence of  $E_0$ .<sup>18</sup> This will be discussed more fully in a later publication.

Theory predicts that phonon scattering determines the positron diffusion constant in relatively pure metals.<sup>23</sup> Since the positron diffusion process has been predicted to be predominantly determined by the positron-phonon interaction, the positron diffusion constant should exhibit a  $T^{-1/2}$  temperature dependence,<sup>23</sup> in reasonable agreement with our experimental value. This is the first direct evidence that the positron diffusion constant in a metal has a negative temperature dependence, although better experimental values await further studies. In this analysis no account has been made for a possible temperature-dependent positron reflection coefficient which might affect the extracted value of  $E_0$  at different sample temperatures. The temperature dependence of this reflection coefficient is determined by the temperature dependence of  $\Phi_p$ , de Broglie wavelength, and the exact shape of the potential at the surface. As the kinetic energy of an incident particle diffusing to an attractive steplike potential approaches zero, the reflection coefficient approaches unity.<sup>22</sup>

The deduced values of  $E_0$  for Al(111) and Al(100) at 300 K are  $2600 \pm 100$  and  $3000 \pm 150$  eV, respectively, when fitting the incident positron energy data which range from 0.025 to 5 keV. One might expect that the mean penetration depth of the positrons would be slightly less in the Al(111) because it is a close-packed layer and this appears to be the case. Mills<sup>5</sup> found  $E_0$  to be  $2860 \pm 150$  eV for Al(100), fitting Eq. (2) without the inclusion of  $\alpha$  and only including incident energy data up to 2 keV. The extracted values for  $E_0$  are dependent on the assumed initial positron distribution and reflection coefficients, therefore, these values have some systematic errors

associated with them. Since the positron mobility is known in Ge at low temperatures,<sup>29</sup> Mills has estimated the constant relating the mean positron depth to the incident energy,  $A$ . His value for  $A$  is  $5.5 \times 10^{-3}$  keV/Å. This number seems reasonable as the range of electrons in Si, determined by depth-resolved cathodoluminescence, was found to be 200 Å at 1 keV, although it exhibited an energy dependence to the 1.6 power.<sup>30</sup> These electron results in Si support our assumption that the mean implant depth is not linear in  $E$  as first suggested by Mills *et al.*<sup>8</sup> Assuming these values of  $A$  are approximately the same for Al as for Si and Ge, one can make a rough estimate of  $D$ . Taking the bulk positron lifetime<sup>31</sup> in Al as  $165 \times 10^{-12}$  sec and an average of the above values for  $A$  and  $E_0$ , one finds  $D$  to be approximately  $0.2$  cm<sup>2</sup>/sec. This is in good agreement with the theoretical prediction of Bergersen *et al.*<sup>23</sup> which is  $0.4$  cm<sup>2</sup>/sec for Al at 300 K. As mentioned, some variation is found in  $E_0$  with different assumed initial positron distributions, therefore, producing an uncertainty in  $D$ . With a Gaussian-shaped initial positron implantation even better agreement is found between theory and the deduced positron diffusion constant. Paulin<sup>32</sup> recently calculated  $D$  in small particles of Al using the positron lifetime, the specific area, and the mass density, and also found a value of  $0.4 \pm 0.2$  cm<sup>2</sup>/sec. McKee *et al.*<sup>33</sup> have estimated  $D$  to be about 2 cm<sup>2</sup>/sec from positron trapping at high-angle grain boundaries in Al. This discrepancy is presently not understood, although in the latter study, complicated metallurgical phenomena may be playing a role. One would expect the range associated with electrons to be an overestimate, as it has been theoretically shown that a positron will lose energy at a higher rate than electrons below 50 eV.<sup>34</sup> Therefore, our estimate with this initial positron distribution should be an upper limit for the diffusion constant.

Figure 4 shows the fitted values of  $\alpha$  in Eq. (2) for Al(111) and Al(100) at various sample temperatures. This type of behavior for  $\alpha$  has been found in other metals.<sup>34</sup> One would expect an approximately constant value, at least up to the onset of positron trapping at vacancies, where this trapping may in fact change the initial positron distribution.<sup>35</sup> This appears to be the case in the temperature range of 423–673 K (Fig. 4). The decrease in  $\alpha$  which approached unity at 163 K is not understood, although this may indicate that diffusion processes play a role in the fitting of the model for the assumed initial positron distribution, or that the positron reflection coefficient increases with decreasing sample temperature.

The decrease in  $\alpha$  at the higher temperatures is attributable to the inadequacy of the model in accounting for positron trapping at thermally generated vacancies in the metal. Another possibility, although

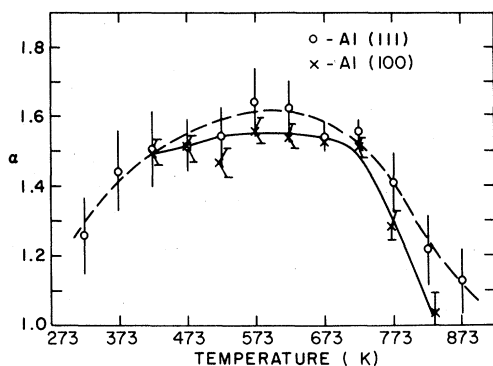


FIG. 4. Deduced values of  $\alpha$  obtained from fitting Eq. (2) to the Al(111) and Al(100) Ps fraction data vs incident positron energy at the corresponding sample temperatures. The errors shown are obtained from the curvative matrix as discussed in Ref. 21.

unlikely, is that prethermalized trapping of the positrons occurs, thus changing the initial positron distribution. For example, a typical nonthermal positron (1 eV) will diffuse on the order of  $30 \text{ \AA}$  in  $1 \times 10^{-12}$  sec while decelerating, which is a significant part of the expected range of low-energy positrons. Thus prethermalized trapping of positrons at monovacancies could produce a significant effect on the initial distribution. Although this is a plausible explanation, a more thorough understanding of this effect will have to await further experiments and a more appropriate approximation of the initial positron distribution.

Both positron trapping at monovacancies and thermally activated detrapping from a surface state can be easily seen by plotting the Ps fraction versus temperature on Al(111) and Al(100), Figs. 5 and 6, respectively. The decrease in the Ps fraction that occurs at the higher temperatures and incident energies, is associated with positron trapping at thermally generated monovacancies. This will be discussed in more detail in Sec. VII.

The initial increase in the Ps fraction (Figs. 5 and 6) is associated with thermal fluctuations capable of detrapping the positron from the surface state and subsequently forming Ps, as discussed by Lynn<sup>10</sup> and Mills.<sup>9</sup> This detrapping energy is intrinsic to clean Al, although as will be shown in the next section the Ps fraction is dependent on surface contamination and adsorbed species. In the studies to date no material has been found from which positrons, not Ps, can escape by this thermally activated process. This finding provides support to the explanation that Ps formation is very dependent on the escape velocity of the positron. Moreover, those positrons that are em-

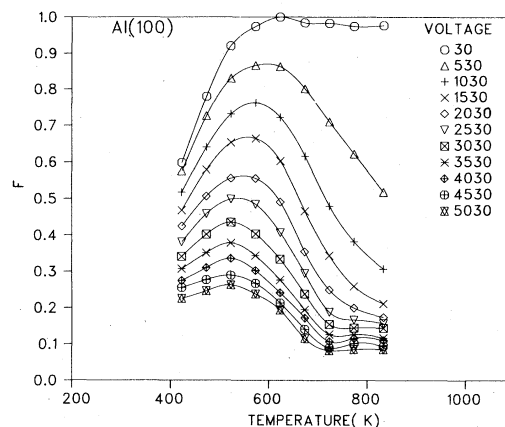


FIG. 5. Fraction of positrons converted to Ps as a function of temperature at different positron energies for Al(100). The solid lines are spline fits through the data points. The negative curvature in the data at the higher sample temperatures and energies is associated with positron trapping at thermally generated monovacancies.

itted are all converted into Ps atoms for  $T \geq 573 \text{ K}$  for Al(100) and  $T \geq 420 \text{ K}$  for Al(111). The reason for this decrease in the positron yield is presently not understood but will most likely include the temperature dependence of the positron work function and, thus, the surface dipole term.

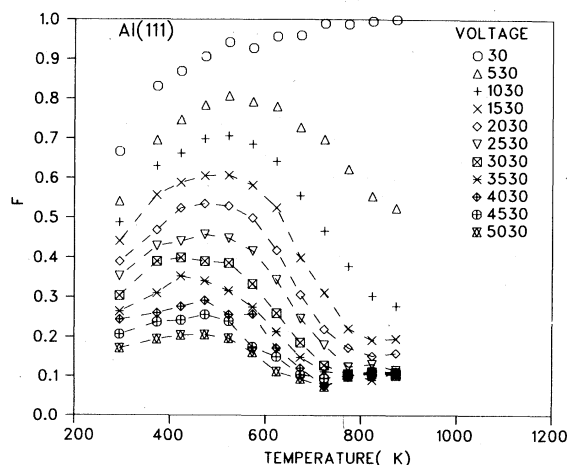


FIG. 6. Ps fraction vs sample temperature at various positron incident energies for Al(111). The dashed lines are spline fits through the data. Positron trapping at thermally generated monovacancies is observed by the negative curvature in the data at the higher sample temperatures and incident energies.

## VI. Ps FRACTION MEASUREMENTS FOR Al(100) AND Al(111) SURFACES AFTER EXPOSURE TO OXYGEN

To better understand the effect of impurities on both the slow-positron yield and the Ps fraction, both the Al(100) and Al(111) surfaces were exposed to ultrahigh-purity oxygen. Aluminum was chosen for these initial studies because the interaction of oxygen with this surface has been of considerable experimental<sup>36</sup> and theoretical<sup>37,38</sup> interest. Aluminum should provide an interesting system for the initial oxidation process since its simple electronic configuration has only *s* and *p* electrons, and technologically Al is the most utilized material for electrodes on semiconductor devices. On the Al(111) plane it has been shown that the initial interaction of oxygen is a two-stage process.<sup>39,40</sup> For less than a monolayer of coverage, the oxygen is dissociatively adsorbed forming a chemisorption phase [ $<200 \text{ L}$  ( $1 \text{ L} = 10^{-6} \text{ torr sec}$ )]. With increased oxygen exposure an intermediate phase develops into a bulklike amorphous  $\text{Al}_x\text{O}_y$ . On the Al(100) face the formation of this oxide layer is much faster and is thought to produce strong surface disorder.<sup>39,40</sup> By studying such systems with positrons it is hoped that new information about defects in the overlayer will be determined. Furthermore, this should provide an initial test of the applicability of slow positrons as a surface probe in chemisorption studies.

The Ps fraction was measured with increasing oxygen exposures up to  $10^6 \text{ L}$ . All the samples were exposed to oxygen at 300 K. In general during the initial stages of oxygen exposure ( $<500 \text{ L}$ ) both the Ps fraction and the normalized oxygen peak of the AES spectra<sup>17</sup> increased in a similar manner. However, in the earliest stages ( $<20 \text{ L}$ ) of oxygen exposure on both Al(111) and Al(100) surfaces a small inflection in the Ps fraction was found. The Al(100) showed this inflection at an exposure of  $\sim 5 \text{ L}$ . This is thought to be an indication of the initial chemisorption ordered phase of oxygen on both Al(111) and Al(100) surfaces.<sup>39,40</sup> This effect will be investigated more thoroughly in a later study. In these measurements different initial coverage rates for the Al(111) and Al(100) were found by AES measurements, and agreed with those published in the literature.<sup>41,42</sup> The changes in the Ps fraction during oxygen exposure closely followed the AES oxygen intensity signal and both the AES signal and the Ps fraction on Al(100) and Al(111) surfaces had been saturated by approximately 300 L exposure.

The Ps yield initially increased with increasing oxygen exposure on the Al(100) surface, most likely indicating that the depth of the positron surface state decreased with increasing oxygen exposure. A second possibility exists where the Ps forms while still residing in the overlayer and subsequently es-

caped into the vacuum before a pickoff process occurs with a spectator electron. In both samples the slow-positron yield decreased with increasing oxygen exposure.

After exposure to 500 L oxygen the Ps fraction increased to approximately 86 and 94% for Al(100) and Al(111), respectively, for an incident positron energy of 25 eV. This exposure ensured more than a full monolayer of oxygen coverage on the Al samples. This demonstrates that Ps formation is associated with the surface and not the bulk properties. Figures 7 and 8 show the Ps fraction versus sample temperature for Al(100) and Al(111) after exposures to 500 L oxygen. At the higher incident energies ( $\geq 1025 \text{ eV}$ ) and temperatures, the general features are the same as for the clean Al (Figs. 5 and 6). In fact, similar monovacancy formation enthalpies are deduced, as will be discussed in Sec. VIII.

One should note the difference in the oxygen-exposed surfaces (Figs. 7 and 8) relative to the clean surfaces (Figs. 5 and 6) in the temperature region of 600–800 K with the low incident energy positrons. The decrease in the Ps fraction which appears in both crystallographic directions indicates that either a potential rise exists at the interface or that trapping centers have been generated in the overlayer which are not allowing the positron or Ps to escape the overlayer. These trapping sites could be generated in the initial stages of the amorphous-to-crystalline phase transition. Since Ps could form in  $\text{Al}_x\text{O}_y$  it is not clear whether these traps are positron or Ps trap-

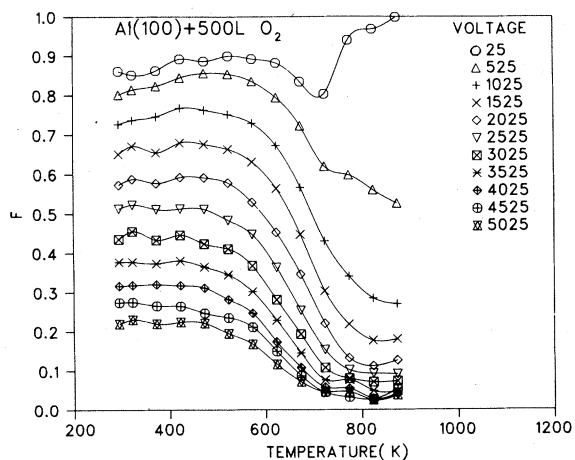


FIG. 7. Fraction of positrons converted to Ps vs sample temperature at various incident positron energies for Al(100) after exposure to 500 L oxygen. The solid lines shown in the figure are produced by a spline fit to the data. The sample remained at each temperature for approximately 15 min. After the high-temperature run the Ps fraction was measured with decreasing temperature and no minimum appeared for the lower-energy positrons in the temperature region between 600 and 800 K.

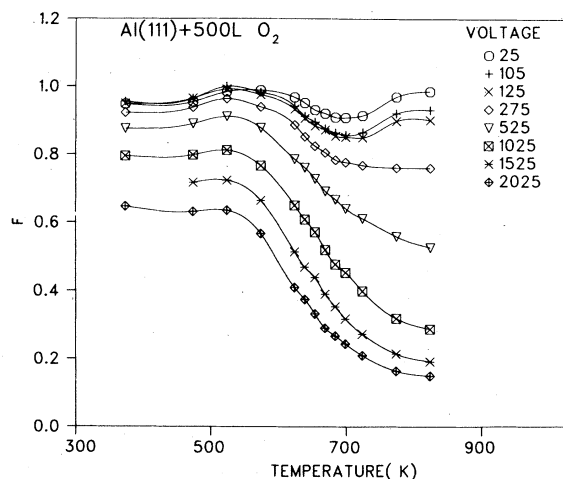


FIG. 8. Ps fraction on Al(111) as a function of sample temperature after exposure to 500 L oxygen. More data points were recorded at other voltages but are not shown in the figure for clarity. After the high-temperature run, no minimum occurred in the Ps fraction with decreasing sample temperature between 600 and 800 K for the lower incident positron energies.

ping centers, although, if Ps is trapped in the overlayer, a spin-exchange process would occur. After this spin-exchange process occurs the Ps ( $^3S_1$ ) atom will then decay by two photons and our measurements will not detect the difference between Ps or positron traps. It is known that for a 30-Å thick oxide layer on Al a phase transition occurs from amorphous to  $\gamma$ - $Al_2O_3$  at approximately 623 K.<sup>36,43</sup> By increasing the sample temperature, the reorientation process to  $Al_2O_3$  continues and concomitantly the traps are removed permitting the Ps or positron to escape more readily into the vacuum. The positron forms Ps during the escape process. After both the Al(100) and Al(111) samples reached their highest temperatures, the measurements were continued at decreasing temperatures and no minimum was found in the Ps fraction, indicating an *irreversible transition*. The Ps fraction versus incident energy data have also been fit to Eq. (2), where similar behavior in  $f_0$  (the Ps fraction formed at  $E = 0$ ) has been found, compared to the low incident positron energies shown in Figs. 7 and 8. After the samples cooled to 300 K, AES intensity measurements were taken and the oxygen peak could still be observed.

To understand this behavior a 5-Å thick oxide layer was grown by exposing the Al(111) sample to  $10^6$  L oxygen.<sup>43</sup> After this exposure, Ps fraction measurements were made versus incident positron energy at increasing sample temperature. These results are shown in Fig. 9. With this  $10^6$  L oxygen

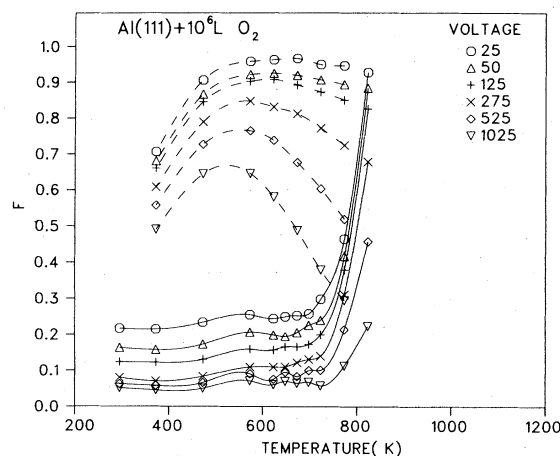


FIG. 9. Fraction of Ps vs sample temperature at various incident positron energies on the Al(111) surface after exposure to  $10^6$  L of ultrahigh-purity oxygen. The solid line is produced by a spline fit to the data points and shows those data taken with increasing sample temperature, whereas the dashed lines indicate those data that were recorded with decreasing temperature. The statistical errors are approximately the size of the data points.

exposure one can observe a large decrease in the Ps fraction, which is most likely associated with positron or Ps trapping in the oxide layer. These measurements start at 300 K and increase with temperature as shown by the solid lines in Fig. 9. The dashed lines show those data that were subsequently recorded with decreasing temperature.

With the lower incident energies ( $\leq 125$  eV) and temperatures greater than 700 K, one can easily observe the large increase in the Ps fraction or concomitantly the decrease in the density of trapping centers in the bulk oxide overlayer. This effect is thought to be attributable to the  $Al_xO_y$  layer and not those defects associated only with the metal-metal-oxide interface. The very-low-energy positrons ( $\leq 25$  eV) should reside mainly in the thin oxide layer. After the transition from amorphous to crystalline  $Al_xO_y$ , Ps forms, indicating that these trapping centers have been removed from this layer. The effect of thermally generated vacancies in the Al is detected with the higher-energy positrons ( $> 275$  eV). As the sample temperature is decreased after the highest temperature is reached, irreversible changes in the Ps fraction occur, consistent with an amorphous-to-ordered transition in the first few atomic layers. With decreasing temperatures ( $< 550$  K) the Ps fraction curves show that an activated process is occurring. This behavior indicates that a positron surface state is found in this ordered overlayer similar to that in metallic systems. From recent photoemission experiments<sup>44</sup> it has been

suggested that this high-temperature crystalline phase of the oxide overlayer is closely related to  $\gamma$ - $\text{Al}_2\text{O}_3$ . This transition was confirmed in this study by LEED measurements after the sample had been cooled, which is in agreement with Martinsson and Flodström.<sup>41</sup>

The Ps fraction versus incident positron energy data were fitted with Eq. (2) and the values obtained for  $E_0$  are consistent with a short positron diffusion length such as that found with trapping centers. The fitted values of  $E_0$  versus temperature are plotted in Fig. 10. The fitted values of  $E_0$  in the oxide layer are a factor of 10 less than the lowest value found for trapping at thermally generated monovacancies in Al, which indicates a significantly higher atomic concentration of trapping centers residing in this amorphous aluminum oxide.

This high-exposure sample was examined under an optical microscope in air after the experimental run. The surface showed signs that when recrystallization occurred some small fraction of the underlying Al was reexposed. The total fraction of exposed surface area associated with this phenomenon should not affect our results.

Presently it is not clear whether these interface states, as determined by photoemission experiments, and the trapping sites for positrons or Ps are directly

related. If Ps is formed in the overlayer, experiments designed to measure the diffusion process and formation rate of these Ps atoms as a function of temperature would prove useful in providing new information on Ps dynamics in condensed solids. Further experimentation with positrons on well-characterized surfaces, coupled with surface techniques such as photoemission, surface soft x-ray absorption, LEED, and AES would provide some of these answers.

## VII. THERMALLY ACTIVATED DETRAPPING OF THE POSITRON FROM A SURFACE STATE

A positron surface trap was first proposed by Mandansky and Rasetti<sup>45</sup> in 1950 to explain their negative results in an attempt to detect the emission of thermal positrons from solids. Positron surface states did not receive theoretical attention until 1973 when Hodges and Stott<sup>24</sup> proposed a model to explain the lack of a Ps signal in voids created by neutron irradiation of metals. In the above communication<sup>24</sup> the analogy was made that a metal-void interface appeared to a positron much like an exterior surface. Furthermore, the long-lived positron lifetime component experimentally observed in voids could be explained by such a surface state. It was suggested<sup>26</sup> that these surface states were in fact the lowest-energy positron states of any type in a metal. After this paper a number of refinements appeared in the literature which included calculations for the transition metals and more recently the inclusion of a dynamic image potential. This latter paper<sup>46</sup> suggests that stable surface states may not exist on all metallic surfaces. In a recent comment by Barberán and Echenique,<sup>47</sup> where the surface-plasmon dispersion and single-particle effects were included in the Nieminen and Hodges<sup>46</sup> model, a reduction of approximately 40% was found in the predicted value for  $E_{ST}$ . In this calculation the dielectric response of the metal is included by a random-phase approximation (RPA), which is known to underestimate the electron-bulk correlation energy as was noted by the authors. Therefore, as the probability increases that the positron wave function extends further inside a metal, i.e., large correlation energies, one would expect a corresponding increase in the binding energy of the positron to the surface state. A measurement of the positron lifetime in a surface state on a well-characterized surface would provide critical information on the nature of this state and would be useful in resolving questions on voids contained in neutron-irradiated samples.<sup>1</sup>

This idealized one-dimensional surface state localizes the positron in the direction perpendicular to the surface and allows translational symmetry parallel to the surface and zero transverse momentum. Any real surface would exhibit potential minima or maxi-

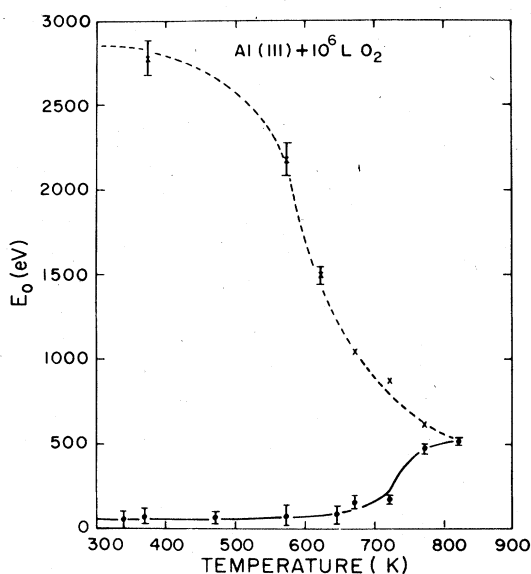


FIG. 10. Temperature dependence of  $E_0$  obtained by fitting Eq. (2) to the data obtained in the Al(111) after exposure to  $10^6$  L oxygen. The error bars shown are obtained from the curvature matrix as discussed in Ref. 21. The solid lines connecting the points were the fits obtained from the data with increasing temperature whereas the dashed lines show those data that were recorded with decreasing sample temperature.

ma at impurity sites or imperfections such as kinks or surface vacancies. These possible variations in the potential on the surface have not been treated theoretically at the present time.

The first slow-positron experiments performed on well-characterized samples were by Mills<sup>5</sup> and showed a strong temperature dependence in the Ps formation for Ge, Si, and Al. It was suggested that some activated process was most likely responsible for the observed temperature dependence in the Ps formation. This confirmed some earlier results of Canter *et al.*,<sup>4</sup> where the surface conditions were unknown. Lynn<sup>10</sup> then showed that data on Ag(111), Ag(100), and Cu(111) could be described by a single activated process which provided evidence for the theoretically predicted surface state. Mills<sup>9</sup> extended the interpretation with a simple Born-Haber cycle so that the binding energy of the positron ( $E_{ST}$ ) to the surface could be extracted. A number of different crystallographic directions in Al, Cu, Cu + S, and Si were measured and it was determined that  $E_{ST}$  ranged from 2 to 3 eV for these metals.<sup>9</sup> More recently Rosenberg *et al.*<sup>7</sup> measured activation energies for Al(100), Ag(polycrystalline), and Ni(100). Other metals such as polycrystalline Ta, Sn(100), and Au(100) showed behavior similar to an activated process.<sup>48</sup> For the remainder of this section the discussion will be centered on Al.

Figure 11 shows the Ps fraction ( $F$ ) versus temperature for Al(111) and Al(100) for a 25 and 40 eV incident energy positron, respectively. A number of the data points have been omitted in these figures for clarity. Low-energy positrons were chosen so that the positron is close to the zero-energy limit and bulk effects, such as thermally generated vacancies, do not need to be considered. This has been checked by comparing plots of  $f_0$ , the  $E = 0$  limit, and good agreement between the measurements was found. In Ag(100), Lynn and Welch<sup>18</sup> found that the extracted activation energies,  $\Delta E$ , associated with the surface were not significantly affected by bulk properties until the positron incident energies were greater than 500 eV, although for Al, bulk effects are apparent at lower incident energies. Some differences do exist between experimentally deduced activation energies.<sup>7,9</sup> In our case a least-squares fit of Eq. (6) to the data yields activation energies for Al(100) and Al(111) of  $0.41 \pm 0.01$  and  $0.33 \pm 0.01$  eV, respectively. On a different Al(100) crystal a value of  $\Delta E = 0.49 \pm 0.01$  eV was obtained with  $C_1$ ,  $C_2$  being approximately a factor of 10 larger. These are compared to Mills's values for Al(100) of  $0.64 \pm 0.02$  eV,<sup>9</sup> for Al(111) of  $0.34 \pm 0.03$  eV and Rosenberg *et al.*<sup>7</sup> value for Al(100) of  $0.44 \pm 0.04$  eV. The extracted values for the Al(111) surface seem to be in good agreement between experiments. Different calibration constants for calculating the Ps fraction ( $R_0$  and  $P_1/P_0$ ) only had a small effect on the ex-

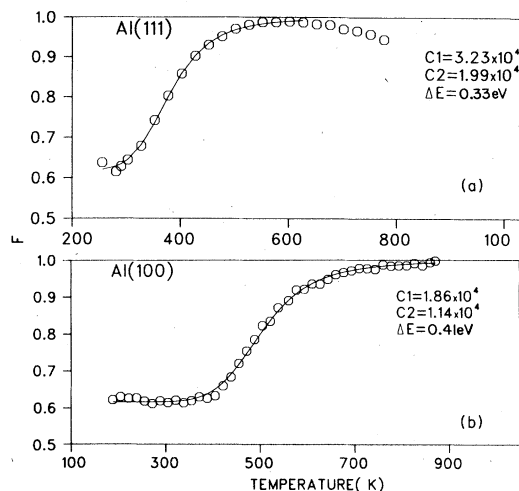


FIG. 11. Fraction of 25- and 40-eV positrons converted to Ps on the Al(111) and Al(100) surface measured as a function of sample temperature, respectively. More data points were recorded but have been omitted for clarity. The solid line is the best fit of Eq. (6) to the data and the values obtained are shown in the figure. Sharp LEED patterns were observed for both the Al(100) and Al(111) samples.

tracted activation energies. These variations in  $\Delta E$  are not presently understood, but might be associated with some type of special site at the crystal surface or the positron emission characteristics. Large changes do occur with the slow-positron emission in the same temperature region as discussed in Sec. IV for the Al(100) sample, which can affect the extracted values for  $\Delta E$ .

It is worthwhile to compare the different experimental values obtained for the pre-exponential term in Eq. (5) divided by the temperature-independent rate for processes competing with thermal activation ( $\Gamma$ ). In Al(100) a value is found for  $\nu/\Gamma$  of  $1.1 \times 10^4$  and for Al(111) a value of  $2.0 \times 10^4$ . These should be compared to Mills's values for Al(100) and Al(111) of  $3.5 \times 10^6$  and  $2.6 \times 10^3$ , respectively. These discrepancies are not understood, although these parameters show a strong correlation in the fitting routine and usually have large errors. Assuming the annihilation rate of a positron residing in the surface state in Al is approximately  $2 \times 10^9 \text{ sec}^{-1}$ , as suggested by Niemenen and Hodges,<sup>46</sup> values of  $\nu$  in our results are found to be  $2.2 \times 10^{13} \text{ sec}^{-1}$  and  $4.0 \times 10^{13} \text{ sec}^{-1}$  for Al(100) and Al(111), respectively. This assumed annihilation rate of the positron in the surface state depends critically on the exact shape of the potential, or in other words, the probability that the positron wave function resides inside the metal, hence experiencing a high electron density. This theoretical value used for the annihilation rate is in

good agreement with those measured experimentally in voids produced in Al by neutron irradiation.<sup>49</sup> These values of  $\nu$  are not unreasonable as  $\nu \cong 10^{15} \text{ sec}^{-1}$  is the oscillation frequency of the 3 eV bound state. Mills<sup>9</sup> suggested that low experimental values of  $\nu$  may indicate a low electron density available for Ps formation. One needs to examine both experimentally and theoretically whether or not a chemisorbed Ps atom exists at any metallic surface. As shown earlier, impurities do play an important role in determining the Ps fraction and will also affect these parameters associated with the surface state in a similar manner. With the present surface-state model this sensitivity to impurities and/or defects is increased as the positron is free to move parallel to the surface. Bulk thermally generated vacancies cannot be responsible for these effects as their concentration is not surface dependent.

Owing to the lack of knowledge of the exact mechanism(s) by which the Ps atoms are emitted, the physical interpretation of the activation energy  $\Delta E$  is somewhat unclear. Mills<sup>9</sup> has used an interpretation based on a Born-Haber cycle to estimate the binding energy of positrons to the surface trap. As shown recently<sup>11</sup> in a measurement of the Ps velocity emitted from a Cu(111) surface at a high temperature, this interpretation appears to be correct. These researchers found the presence of thermal ( $\sim 0.1$  eV) Ps atoms emitted at high sample temperature ( $\sim 790^\circ\text{C}$ ) and a nonthermal emission process ( $\sim 3$  eV) at  $30^\circ\text{C}$ . Assuming that Ps does not exist as a chemisorbed atom, one can then suppose that a positron is thermally desorbed from the potential well at the surface. Certainly variations in the potential well at the surface or interaction with surface electron states will play a role and are not considered in this simple Born-Haber interpretation. For example, the rate of formation for Ps near the surface is not known and should play a role in the escape process. The energy required to remove positrons from this surface state to rest at infinity is the binding energy,  $E_{\text{ST}}$  as described by Eq. (8). As mentioned by Lynn and Welch<sup>18</sup> this must be a lower limit, as it may be necessary to excite the trapped positron to a larger energy, so that at a significant distance from the surface Ps can form in the low electron density limit.<sup>2</sup> In fact it has been theoretically predicted that the Ps binding energy is very strongly dependent on the electron density.<sup>2</sup> Therefore, based on this Born-Haber cycle the surface trap depth is less than the sum of the terms on the right-hand side of Eq. (8).

The electron work functions,  $\Phi_e$ , for Al(111) and Al(100) have been recently reported as  $4.23 \pm 0.02$  and  $4.36 \pm 0.02$  eV, respectively.<sup>42</sup> Assuming that those Ps atoms which are emitted into the vacuum at low temperatures ( $\sim 300$  K) are not involved in any inelastic loss processes, one can estimate  $\Phi_{\text{Ps}}$  by Eq. (9) as being  $-2.9$  and  $-2.7$  eV for Al(111) and

Al(100), respectively. These Ps emission energies can now be checked by using the method of Ref. 11 and will be reported in a later publication.

Using Gartland's<sup>42</sup> values for the electron work function in Eq. (8) and the experimentally determined  $\Delta E$ 's one finds  $E_{\text{ST}}$  to be less than 2.77 and 2.98 eV, for Al(111) and Al(100), respectively. Our present values appear to be higher than Nieminen and Hodges's theoretically predicted value of 2.1 eV for Al.<sup>46</sup>

It is noteworthy that if one assumes for a particular metal that the sum of the positron and electron work functions is a constant, then the positron work function on the clean Al(111) sample would be a less negative value. For example, using Gartland's<sup>42</sup> values for the electron work function the sum ( $\Phi_e + \Phi_p$ ) for Al(100) is approximately 4.15 eV, therefore the positron work function for the Al(111) should be  $-0.07$  eV in agreement with our extracted value.<sup>35</sup> This could also explain the low slow-positron yield observed in the Al(111) crystal, as the probability of Ps formation increases as the positron work function becomes less negative. More data are needed to confirm this hypothesis.

Extending this simple picture to oxygen exposure on Al(111) Gartland found that the Al(111) electron work function increased and appeared to saturate after 100 L at 4.33 eV and the Al(100) decreased to approximately 3.9 eV after exposure to approximately 200 L of oxygen.<sup>42</sup> Assuming nothing catastrophic occurs in the Al(111) electron work function between 200- and 500-L oxygen exposure, the Born-Haber model seems to be in disagreement with these measurements, as the Ps fraction is increasing instead of decreasing or staying at a constant as suggested by Eq. (8). However, Bradshaw *et al.*<sup>50</sup> found that changes in the electron work function on Al(111) depended strongly on sample-preparation conditions and in their study a decrease of 0.18 eV was found, which would be consistent with our findings. Before a firm conclusion can be reached, more measurements are necessary to determine whether the electron work function does increase on our Al(111) sample with oxygen exposure or whether Ps forms while residing at the surface.

The Ps fraction increased, excluding a small inflection that occurred at low exposures ( $< 20$  L), with increasing oxygen exposures up to 500 L at 298 K. As previously mentioned, this increase could also be explained if the formation of Ps occurred before the positron diffused through the surface. The increase in the Ps fraction with oxygen coverage ( $< 500$  L) did follow more closely that of the AES oxygen signal and not the electron work-function changes measured by Gartland<sup>42</sup> or Bradshaw *et al.*<sup>50</sup> As can be seen in Figs. 7 and 8, there is no temperature-activated Ps emission at least above 300 K. Low-temperature measurements are presently being considered to

resolve the question of an activated process. It appears that the initial exposure to oxygen increases the Ps fraction by allowing the positron to be easily detrapped from the surface state (low binding energy) or that Ps forms before escaping into the vacuum. The probability of trapping the positron in the surface state could be significantly reduced, owing to the oxide formation on the surface, and should have the kinetic energy distribution characteristic of the Ps work function<sup>51</sup> of this oxide. If the positrons are thermally detrapped at 300 K and form Ps, a kinetic energy spread corresponding to a thermal distribution should be found for those positrons thermally desorbed. Ps energy-distribution measurements after exposing the Al to oxygen are necessary to ascertain the correct physical interpretation.

### VIII. EXTRACTION OF THE VACANCY FORMATION ENTHALPY FROM THE Ps DATA

The use of slow-positron beams in measuring bulk properties such as the vacancy formation enthalpy or defect properties residing near the surface has a number of advantages over the more standard bulk positron measurements. Bulk measurements which employ a radioactive salt as a direct positron source, have been severely limited to measuring only those systems where thick samples could be fabricated, thus ensuring that the positrons stop in the material under study. This slow-positron method can use sample thicknesses on the order of 1  $\mu\text{m}$ . In the present measurements an effective diffusion length of the positron is measured whereas in bulk positron experiments only positron lifetime or momentum profiles can be extracted. The latter are usually sufficient, although a positron can conceivably trap in a lattice defect without significantly changing either of these properties relative to the perfect lattice.

This technique also has the advantage that no source contribution is present as in the case when a radioactive salt is placed directly on the sample for bulk measurements. This correction for bulk measurements produces some uncertainty in the data analysis used in determining the monovacancy formation enthalpy. Another consideration is that the metals studied by the slow-positron technique up to the present, Ag, Cu, and Al, show no signs of a temperature-dependent effect before the onset of detectable positron trapping at thermally generated vacancies, as has been seen in most of the standard bulk positron techniques. This temperature-dependent effect ("prevacancy effect") has created considerable difficulty in extracting accurate defect information and its origin is not fully understood at the present time.<sup>1</sup> Although many uncertainties still exist with the present method it should certainly ex-

pand the applicability of the positron technique in the study of materials containing vacancy-type defects.

In the present method deduced values of  $E_0$  are obtained by performing a least-squares fit of Eq. (2). These values are then fit with Eq. (4). Although a number of assumptions<sup>18</sup> have gone into the derivation of Eq. (4), one does find reasonable agreement with other experimental values.<sup>52</sup> Figure 12 shows a typical set of data for  $E_0$  with the solid line representing the best fit of Eq. (4) through the data. The vacancy formation enthalpy extracted from these measurements,  $E_{IV}^f = 0.61 \pm 0.05$  eV, is in reasonable agreement with those extracted from bulk positron measurements which range from 0.62 to 0.66 eV.<sup>52</sup> The analysis procedure was also performed with different values of  $R_0$  and assumed initial positron distribution profiles.<sup>35</sup> Only a small change was found in  $E_{IV}^f$ , indicating the general applicability of this model. From measurements in Ag and Cu (Ref. 18) one also finds reasonable agreement, although the formation enthalpies are also slightly lower than the widely adopted bulk values.

Figure 13 shows the values of  $E_0$  versus temperature from which a formation enthalpy of  $0.62 \pm 0.05$  eV was extracted for Al(100) after exposure to 500 L oxygen. This is included to demonstrate that the formation enthalpy is not determined by impurities on the surface. A vacancy formation enthalpy of  $0.65 \pm 0.05$  eV was also found for Al(111)-500 L oxygen, in reasonable agreement with the other values. The differences between the formation enthalpies are attributable to both statistical and systematic errors. It should be mentioned that for larger fitted values for  $E_0$ , such as with Cu,<sup>18</sup> a strong correlation with  $f_0$

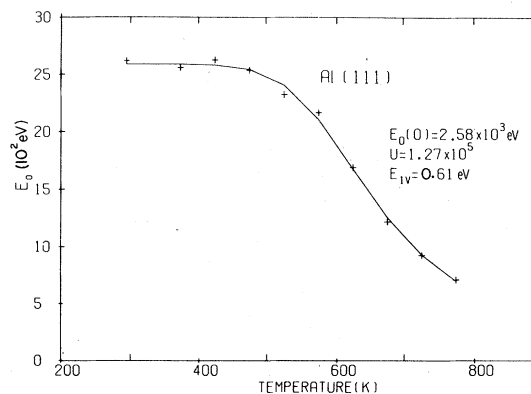


FIG. 12. Temperature dependence of  $E_0$  obtained from fitting Eq. (2) to the Al(111) Ps fraction data vs incident positron energy. The solid line is the best fit of Eq. (4) through the data at the corresponding temperatures. The extracted values are shown in the figure where  $E_{IV}^f$  and  $E_0(0)$  are in eV.



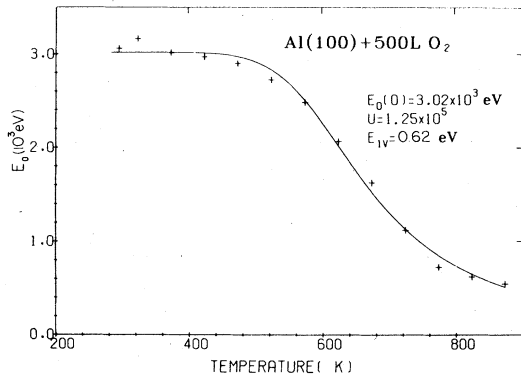


FIG. 13. Temperature dependence of  $E_0$  obtained from the least-squares fit of Eq. (2) to the Ps fraction data vs incident positron energy for Al(100) exposed to 500 L oxygen. The solid line is the best fit of Eq. (4) through these deduced values of  $E_0$  vs temperature.

exists which can produce a significant error in the deduced formation enthalpies.

In various experimental runs on Al,  $U$  of Eq. (4) varies from  $1.3-5 \times 10^5$ . By dividing this quantity by the bulk positron lifetime in Al ( $165 \times 10^{-12}$  sec),<sup>31</sup> one finds  $\mu \exp(S_V^f/k)$  to be  $8 \times 10^{14}-3 \times 10^{15}$  sec<sup>-1</sup>. The range of values is in good agreement with those that have been determined by bulk positron measurements,<sup>1,52</sup> in support of the model. In fact, this technique should be very useful in determining the nature of defects in thin films, ion-implanted, laser-annealed samples, and overlayers on semiconductor or metal samples.

## IX. CONCLUSIONS

Clean Al(111) and Al(100) surfaces and those exposed to oxygen have been examined with monoenergetic positrons for a variety of incident energies and sample temperatures. Significant slow-positron emission was observed on the Al(100) surface and to a lesser extent on the Al(111) surface. The slow-positron yield was found to be both temperature and incident energy dependent. The slow-positron yield decreased approximately to zero with exposure to 500 L oxygen on both surfaces.

A single thermally activated detrapping process adequately describes the Ps fraction data for low in-

cident energy positrons for both the Al(100) and Al(111) surfaces. A model was used to deduce the activation energies which were then used to estimate the binding energy of the positron to the surface ( $E_{ST} \leq 3$  eV). The Ps fraction increased during the initial exposure of oxygen indicating that a larger fraction of Ps could be emitted directly into the vacuum or that the binding energy to the surface trap was reduced significantly to allow detrapping to occur at 300 K. At large oxygen exposures ( $\sim 10^6$  L O<sub>2</sub>), trapping centers for positrons of Ps were found to reside in the overlayer of amorphous Al<sub>x</sub>O<sub>y</sub>, thus reducing the positron diffusion length and therefore the Ps fraction. As the crystal was heated, the amorphous-to-crystalline surface transition of Al<sub>x</sub>O<sub>y</sub> was signaled by the decrease in the concentration of positron- or Ps-trapping sites. This method should be useful in studying those defects residing in thin films and overlayers and should provide useful information, of both fundamental and technological interest, on interfaces.

Rough estimates were made of both the temperature dependence and the absolute value of the positron-diffusion constant and were found to be in reasonable agreement with theoretical predictions. The vacancy formation enthalpy was deduced from the clean and oxygenated (500 L) samples showing the applicability of this technique for the study of thin films. The enthalpies extracted from the fit of the model to the data are in good agreement with those values reported from bulk positron studies. The monovacancy specific trapping rates for positrons were deduced and compare well with those from bulk positron measurements. The future of slow positrons as an effective surface probe awaits a theoretical understanding of both the formation process of Ps and the temperature dependence of the positron work function and yield.

## ACKNOWLEDGMENTS

The authors would like to thank A. Goland, Y. C. Jean, H. Jorch, and D. O. Welch for useful discussions, M. McKeown for computer assistance, and M. Carroll and J. Hurst for technical support. K.G.L. would like to thank Los Alamos Scientific Laboratory for their support and hospitality while this manuscript was being written.

\*Present address: Div. of Neurological Surgery, Medical College of Virginia, Richmond, Virginia 23298.

<sup>1</sup>A number of reviews are available, the most recent being *Positrons in Solids*, edited by P. Hautojärvi (Springer-Verlag, New York, 1979).

<sup>2</sup>Joseph Callaway, *Phys. Rev.* **116**, 1140 (1959); A. Held

and S. Kahana, *Can. J. Phys.* **42**, 1908 (1964); D. N. Lowy and A. D. Jackson, *Phys. Rev. B* **12**, 1689 (1975).

<sup>3</sup>P. G. Coleman, T. C. Griffith, and G. R. Heyland; *Appl. Phys.* **4**, 89 (1974); W. E. Kauppila, T. S. Stein, G. Jenson, M. S. Sababneh, and V. Pol, *Rev. Sci. Instrum.* **48**, 822 (1977), and references therein.

- <sup>4</sup>K. F. Canter, A. P. Mills, Jr., and S. Berko, *Phys. Rev. Lett.* **33**, 7 (1974).
- <sup>5</sup>A. P. Mills, Jr., *Phys. Rev. Lett.* **41**, 1828 (1978).
- <sup>6</sup>K. G. Lynn, *J. Phys. C* **12**, L435 (1979).
- <sup>7</sup>I. J. Rosenberg, A. H. Weiss, and K. F. Canter, 26th National Symposium of the American Vacuum Society, 1979 (unpublished).
- <sup>8</sup>A. P. Mills, Jr., P. M. Platzman, and B. L. Brown, *Phys. Rev. Lett.* **41**, 1076 (1978); K. G. Lynn and H. L. Lutz, *Am. Phys. Soc.* **24**, 271 (1979).
- <sup>9</sup>Allen P. Mills, Jr., *Solid State Commun.* **31**, 623 (1979).
- <sup>10</sup>K. G. Lynn, *Phys. Rev. Lett.* **43**, 391 (1979); **43**, 803(E) (1979).
- <sup>11</sup>A. P. Mills, Jr., and Loren Pfeiffer, *Phys. Rev. Lett.* **43**, 1961 (1979).
- <sup>12</sup>K. G. Lynn, *Phys. Rev. Lett.* **44**, 1330 (1980).
- <sup>13</sup>A full description of the experimental apparatus to be published, K. G. Lynn and H. Lutz, *Rev. Sci. Instrum.* (in press).
- <sup>14</sup>A. P. Mills, Jr., *Appl. Phys. Lett.* **36**, 427 (1979).
- <sup>15</sup>A. Ore and J. L. Powell, *Phys. Rev.* **75**, 1696 (1976).
- <sup>16</sup>S. Marder, V. W. Hughes, C. S. Wu, and W. Bennett, *Phys. Rev.* **103**, 1258 (1956).
- <sup>17</sup>Physical Electronic Industries, *Handbook of Auger Electron Spectroscopy* (unpublished).
- <sup>18</sup>K. G. Lynn and D. O. Welch, *Phys. Rev. B* **22**, 99 (1980).
- <sup>19</sup>Allen P. Mills, Jr., and Cherry A. Murray, *Appl. Phys.* **21**, 323 (1980).
- <sup>20</sup>A. F. Makhov, *Sov. Phys. Solid State* **2**, 1934 (1960).
- <sup>21</sup>Philip R. Bevington, *Data Reduction and Error Analysis for the Physics Sciences* (McGraw-Hill, New York, 1969).
- <sup>22</sup>J. Oliva, *Phys. Rev. B* (in press); see also L. D. Landau and E. M. Lifshitz, *Quantum Mechanics* (Pergamon, New York, 1977).
- <sup>23</sup>B. Bergersen, E. Pajanne, P. Kubica, M. J. Stott, and C. H. Hodges, *Solid State Commun.* **15**, 1377 (1974).
- <sup>24</sup>C. H. Hodges and M. J. Stott, *Solid State Commun.* **12**, 1153 (1973); R. M. Nieminen and M. Manninen, *ibid.* **15**, 403 (1974).
- <sup>25</sup>R. M. Nieminen and J. Lakkonen, *Appl. Phys.* **20**, 181 (1979).
- <sup>26</sup>C. H. Hodges and M. J. Stott, *Phys. Rev. B* **7**, 73 (1973); R. M. Nieminen and C. H. Hodges, *Solid State Commun.* **18**, 1115 (1976).
- <sup>27</sup>J. B. Pendry, *J. Phys. C* (in press).
- <sup>28</sup>B. Bergersen and E. Pajanne, *Appl. Phys.* **4**, 25 (1974).
- <sup>29</sup>A. P. Mills, Jr., and L. Pfeiffer, *Phys. Rev. Lett.* **36**, 1389 (1976).
- <sup>30</sup>C. E. Barnes (private communication).
- <sup>31</sup>K. G. Lynn, J. E. Dickman, W. L. Brown, M. F. Robbins, and E. Bonderup, *Phys. Rev. B* **20**, 3566 (1979).
- <sup>32</sup>R. Paulin, in *Proceedings of the Fifth International Conference on Positron Annihilation*, Japan, 1979 (unpublished).
- <sup>33</sup>B. T. A. McKee, A. T. Stewart, L. Morris, and H. Sang, in *Proceedings of the Fifth International Conference on Positron Annihilation*, Japan, 1979 (unpublished).
- <sup>34</sup>R. H. Ritchie and J. C. Ashley, *J. Phys. Chem. Solids* **26**, 1689 (1965).
- <sup>35</sup>K. G. Lynn (unpublished data).
- <sup>36</sup>Antonio Bianconi, R. Z. Bachrach, and S. A. Flodström, *Phys. Rev. B* **19**, 3879 (1979), and references therein.
- <sup>37</sup>N. D. Lang and A. K. Williams, *Phys. Rev. Lett.* **34**, 531 (1975).
- <sup>38</sup>I. P. Batra and S. Cirace, *Phys. Rev. Lett.* **39**, 774 (1977).
- <sup>39</sup>W. Eberhardt and F. J. Himpsel, *Phys. Rev. Lett.* **42**, 1375 (1979).
- <sup>40</sup>S. A. Flodström, C. W. B. Martinsson, R. Z. Bachrach, S. B. M. Hagstrom, and R. S. Bauer, *Phys. Rev. Lett.* **40**, 907 (1978).
- <sup>41</sup>C. W. B. Martinsson and S. A. Flodström, *Surf. Sci.* **80**, 306 (1979).
- <sup>42</sup>P. O. Gartland, *Surf. Sci.* **62**, 183 (1977).
- <sup>43</sup>D. S. Campbell, in *Handbook of Thin Film Technology*, edited by L. I. Missel and Glang (McGraw-Hill, New York, 1970).
- <sup>44</sup>A. Balzarotti, A. Bianconi, E. Burattini, G. Grandolfo, R. Habel, and M. Piacentini, *Phys. Status Solidi B* **63**, 77 (1974).
- <sup>45</sup>L. Madansky and F. Rasetti, *Phys. Rev.* **79**, 397 (1950).
- <sup>46</sup>R. M. Nieminen and C. H. Hodges, *Phys. Rev. B* **18**, 2568 (1978).
- <sup>47</sup>N. Barberán and P. M. Echenique, *Phys. Rev. B* **19**, 5431 (1979).
- <sup>48</sup>K. G. Lynn (unpublished data).
- <sup>49</sup>K. Petersen, N. Thrane, G. Trumpy, and R. W. Hendricks, *Appl. Phys.* **10**, 85 (1976).
- <sup>50</sup>A. M. Bradshaw, P. Hofmann, and W. Wyrobisch, *Surf. Sci.* **68**, 269 (1977).
- <sup>51</sup>C. H. Hodges and M. J. Stott, *Phys. Rev. B* **7**, 73 (1972); R. M. Nieminen and C. H. Hodges, *Solid State Commun.* **18**, 1115 (1976).
- <sup>52</sup>M. J. Fluss, L. C. Smedskjaer, M. K. Chason, D. G. Legnini, and R. W. Siegel, *Phys. Rev. B* **17**, 3444 (1978), and references therein.